J. Applied Membrane Science & Technology, Vol. 28, No. 3, December 2024, 59–84

Reuse of End-of-life Seawater Reverse Osmosis (RO) Membranes for Water Treatment

Noor Al-Hamimi[a,b], Htet Htet Kyaw[a], Buthayna Al-Ghafri[a], Sulaiman Al-Obaidani[c], Jauad El Kharraz[d], Khaled Al-Anezi[e] & Mohammed Al-Abri[a,b*]

[a]Nanotechnology Research Center, Sultan Qaboos University, P.O. Box 33, Al-Khoudh, Muscat 123, Oman
[b]Department of Petroleum and Chemical Engineering, College of Engineering, Sultan Qaboos University, P.O. Box 33, Al-Khoudh, Muscat 123, Oman
[c]Department of Mechanical and Industrial Engineering, Sultan Qaboos University, P.O. Box 33, Al-Khoudh P.C. 123, Oman
[d]Regional Center for Renewable Energy and Energy Efficiency (RCREEE), Egypt
[e]Chemical Engineering Technology Department, College of Technological Studies (CTS), Kuwait City, Kuwait

Submitted: 30/10/2024. Revised edition: 5/12/2024. Accepted: 8/12/2024. Available online: 12/12/2024

ABSTRACT

Due to the continuing growth in RO desalination plants and the finite lifespan of the RO membranes, large stocks of the end-of-life (EoL) RO membranes are discarded to landfills. This has become a critical challenge in the RO desalination industry. The overall objective of this study was to validate the possibility of direct reuse of the end-of-life seawater reverse osmosis membranes (EoL SWRO) for brackish water desalination in order to limit the environmental impact of their disposal. This study investigates the membrane performance and characterization of four SWRO modules (EoL-M1, EoL-M2, EoL-M3, and EoL-M4). The hydraulic performance of the old membranes was assessed using 5,000 ppm synthetic (NaCl) brackish water and real brackish water, and was compared with the performance of two commercial membranes, namely brackish water RO membrane (BW30) and nanofiltration membrane (NF90). 84-92% NaCl rejection was achieved by direct reuse of EoL membranes, which was higher than the rejection characteristics obtained using commercial BW30 and NF90 membranes. Removal of common salts represent in natural water sources (Na_2SO_4, Mg_2SO_4 and $MgCl_2$) and humic substances was also investigated using EoL membranes. The rejection of Na_2SO_4, $MgSO_4$ and $MgCl_2$ salt solutions was in the range of (50.0-85.8%) with a highest rejection value was obtained for Na_2SO_4 and the lowest rejection was observed for $MgCl_2$ solution, while a complete rejection was achieved for humic acid. Salt rejection of real brackish water filtration by the EoL membranes (75-77%) presented NF-like properties (Salt rejection was obtained for NF90 membrane was 77%). Therefore, the potential of reusing EoL SWRO is promising and thus benefit the desalination industry and the environment in Oman.

Keywords: Reverse osmosis, end-of-life membranes, desalination, brackish water, environmental impact, reuse

1.0 INTRODUCTION

The demand for freshwater has been increasing on a global scale [1-4]. Many countries are expected to face critical water shortages by 2050, and Oman is one of them [2, 5]. In recent years, numerous desalination plants have been built to cover the increased demand for freshwater [6]. Reverse osmosis (RO)

* Corresponding to: Mohammed Al-Abri (email: alabri@squ.edu.om)
DOI: https://doi.org/10.11113/jamst.v28n3.306

membrane technology dominates the desalination market nowadays, holding 65% [2] of the currently installed desalination capacity around the world, with more than 10,000 installations of various RO sizes [3, 5, 7, 8].

The operational lifespan of RO membranes, e.g., the stability of the permeate flux and salt retention, is finite and is dependent on the feed water quality, operating conditions, type of membrane and cleaning routine. Feed water pretreatment and regular cleaning of membranes are the most common practices applied to extend the lifetime of RO membranes [9]. However, there are many factors contributing to the decline of membrane performance over its lifetime including; irreversible membrane fouling and degradation of the active membrane layer [1, 2, 8, 10]. Routine cleaning processes are commonly carried out in desalination plants (with oxidative solutions, acids and bases), in order to restore the permeate flux [9]. However, with long-term operation of RO systems, the repetitive and incidental exposure of membranes to cleaning and antifouling agents degrade the active polyamide (PA) layer of RO membranes causing a loss in membrane performance [8, 11]. A general review of membrane technology reports a replacement rate of commonly 10-20 % per year (Every 2-5 years) for seawater applications and between 5-10 % per year (Every 5-7 years) for brackish water applications [2]. However, this is highly dependent upon the operating conditions of RO system and the quality of feed water [10, 11]. These damaged membranes are known as end-of-life (EoL) membranes which are defined as used membranes that have been removed from their primary applications due to irreversible decline in their performance [10-12].

Large stocks of EoL RO membranes have accumulated over the years due to the continuing growth of RO desalination [10, 12-14]. An estimate of >840,000 old RO modules are discarded annually worldwide considering that >5.6 million seawater RO modules are installed in 150 countries [15], with an average replacement rate between 10 and 20% per year. This is equivalent to >14,000 tons of plastics assuming an average weight of 17 kg per EoL RO module. This is a critical issue, that will only get worse in the future [2]. Currently, EoL RO membranes are considered as waste and are generally incinerated or disposed in local landfills. The disposal of EoL RO membranes is emerging as a primary environmental concern leading to a significant environmental impact [2, 8, 11, 14, 16].

Alternative options can be considered for EoL membranes in order to manage their landfill disposal; one possible solution involves direct reuse of EoL seawater RO membranes within lower salinity feed systems like brackish water desalination, seawater pretreatment and wastewater treatment. Other options include: direct recycling of EoL membranes by chemical conversion into NF or UF membranes, indirect recycling; whereby RO membranes are unrolled then recycled [2, 8, 10, 12, 13]. Another alternative for EoL membranes includes the use of RO modules with different performances within the same pressure vessel in order to optimize the overall process efficiency [11]. Among all of these alternatives, direct recycling is the most studied process [2].

Direct reuse of EoL membranes offers a great promise in water treatment industry. However, a small number of studies identified the direct reuse potential of these EoL membranes. Direct reuse refers to the use of EoL membranes that were considered unsuitable for their primary application within a secondary

application [2]. Ould *et al*. [17] investigated the opportunity to directly reuse EoL seawater RO membranes followed autopsy procedure to determine the permeability and salt rejection of discarded RO membranes using synthetic NaCl solution. Based on the values of the solute concentration observed for the permeate due to convection (C_{conv}) for the tested virgin and used membranes, the authors concluded that the tested EoL RO membranes had NF membranes properties [17]. They found that the C_{conv} values observed for the virgin RO membranes were close to zero while the value of the same parameter (C_{conv}) was 1.8 g/L for the old membranes which means that solute transport through RO membranes occurred only by pure diffusion. Therefore, by considering that in NF process solute transfer occurs by diffusion and convection and in ultrafiltration process (UF) solute transfer occurs only by pure convection, they approved that the tested old SWRO membranes are well NF membranes. Prince *et al*. [18] compared the performances of old brackish water RO (BWRO) membranes to those reported for new membranes using synthetic NaCl solution. The performance testing was conducted at a pressure of 15.5 bar. It was shown that although all tested membranes were no longer in accordance with the manufacturer's performance criteria of 99.5% rejection, all sampled membranes showed more than 96% salt rejection [18]. Moreover, Kraemer and Rosa [19] studied the direct reuse of discarded RO membranes, after water demineralization processes, in the treatment of a cooling tower effluent in a petrochemical company. The permeate of this process was utilized as a makeup water for the cooling tower.

The main objective of this work is to investigate the possibility of direct reuse of EoL seawater RO membranes for brackish water treatment. Different water qualities have been assessed to evaluate the hydraulic performance of the EoL membranes. Results are compared with commercial BW30 RO and NF90 nanofiltration membranes. Furthermore, surface characterization of the EoL membranes was also performed using different characterization techniques.

2.0 MATERIALS & METHODOLOGY

2.1 Materials and Membranes

Sodium Chloride (NaCl, BDH, England), Sodium Sulphate anhydrous (Na_2SO_4, Sigma Aldrich, Germany), Magnesium Sulphate hepta-hydrate ($MgSO_4.7H_2O$, Merck, Germany) and Magnesium Chloride ($MgCl_2$, Sigma Aldrich, Germany) synthetic solutions were prepared by mixing the required quantity of each salt with deionized water to achieve a concentration of 5,000 mg/L. Humic acid solution (10 mg/L) was prepared by dissolving 10 mg of commercially available humic acid powder (Sigma-Ardrich) in 1L of ultrapure water.

EoL membranes were cleaned prior to being analyzed or reused. Cleaning was performed by immersion using a combined acid-base chemical cleaning using 6% w/v sodium hydroxide (NaOH, pH 11) and 6% w/v citric acid (pH 4) solutions. Membranes were preserved in deionized water for 30 minutes before and after each cleaning step. Sodium hydroxide purchased from Sigma Aldrich was prepared by diluting a commercial product (6 g of NaOH) in 100 ml of deionized water. Citric acid purchased from Merck company was prepared by diluting the commercial reagent with deionized water (6 g of citric acid in 100 ml of deionized water)

and supplemented with sulphuric acid to lower the pH to 4. These solutions were stored in two containers to be used for all cleaning processes.

All tests were performed on EoL thin-film composite (TFC) PA RO membranes, which were cut from different 8" spiral wound modules discarded from seawater desalination plants in Oman (Figure 1). Flat sheet membrane samples with different levels of fouling, chemical and/or physical damage were cut from each membrane module in order to conduct membrane performance test and membrane surface characterization (with or without cleaning, depending on characterization type and research requirements). The used end-of-life SW30HR DOW Filmtec RO membrane modules are classified as follows; EoL-M1, EoL-M2, EoL-M3 and EoL-M4. The performance of these EoL membranes was compared with commercial brackish water RO (BW30) and NF (NF90) membranes. Moreover, the commercial SW30HR RO membrane was used to compare the surface characteristics of the used EoL membranes with the properties of the commercial membrane. DOW Filmtec virgin membranes were purchased from Sterlitech Corporation. The specifications of the commercial SW30HR, BW30 and NF90 membranes is shown in Table S1, supporting information. Membrane samples were characterized using several methods in order to understand the relationship between structure and properties of the top layer with membrane performance.

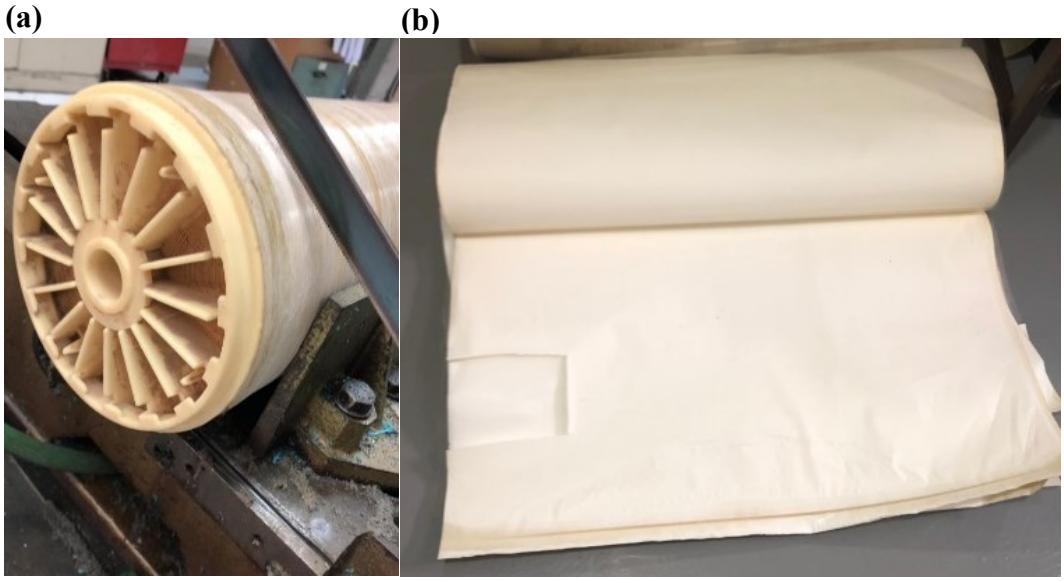

Figure 1 (a) Dissection of EoL membrane module and (b) Extraction of EoL membranes flat sheets

2.2 Membranes Characterization

The surface morphology of all membranes was characterized using a field emission scanning electron microscopy (FESEM, JEOL JSM-7600F) operated at accelerated voltage of 20 kV. The membranes were dried for two days in an electronic desiccator (SECADOR DESICCATOR, USA) prior to the SEM analysis. Energy dispersive X-ray spectroscopy (EDS) was coupled with SEM analysis (Oxford instruments (X-Max, UK)

detectors and data were interpreted by AZtec nanoanalysis software) to examine the chemical content of the membrane surface. EoL seawater RO membranes were characterized by attenuated total reflection-Fourier transform infrared (FTIR) spectroscopy using a PerkinElmer, FT-IR spectrometer. The spectra were recorded at a resolution of 4.0 cm^{-1} in the frequency region of 4000–500 cm^{-1}, with an average of 32 scans per sample. Previously the samples were dried for two days in an electronic desiccator (SECADOR DESICCATOR, USA) to remove moisture. Membrane fouling of EoL membranes was identified by Thermal Gravimetric analysis (TGA) using Perkin Elmer (STA 6000) analyzer under inert atmosphere using N_2 gas. The experiments were conducted at a heating rate of 10 °C/min and a gas flow of 20 ml/min from 25 °C to 800 °C. Nitrogen gas purging was applied for 5 minutes prior to the experiment. Static contact angles of membranes were determined with Optical Theta Lite attention tensiometer instrument (Biolin Scientific, Sweden) using the sessile drop technique. All membrane samples were fixed on microscopic glass supports, then 5-µL of deionized water (DI) water was placed on the membrane surface using a Hamilton syringe at 25 °C. Five different places that were randomly chosen on the membrane surface were acquired to yield an average result of the contact angle. EoL membrane samples were cleaned and then dried for two days before contact angle analysis in an electronic desiccator (SECADOR DESICCATOR, USA). X-ray photoelectron spectroscopy (XPS) spectra were conducted using an Omicron Nanotechnology XPS system. A monochromatic Al Kα radiation (hν= 1486.6 eV) of source voltage 15 kV and an emission current of 20 mA was employed for analysis. All scans were conducted at a base pressure of ~ 10^{-10} mbar. The composition of the sample was extracted from the wide scan while the individual element peaks were recorded at constant analyzer transmission energy of 20 eV. As charging effects are unavoidable in the XPS study of non-conducting samples, charge compensation was performed by electron gun flooding. The obtained XPS spectra were deconvoluted to their individual components using Gaussian Lorentzian function after background subtraction with Shirley function in Casa XPS software (Casa Software Ltd, UK). The binding energies were calibrated with respect to adventitious C 1s feature at 284.6 eV.

2.3 Membrane Setup and Performance

A laboratory-scale reverse osmosis system operates in a cross-flow configuration was used to carry out the end-of-life membranes performance characterization. The cross flow system comprised of a 15 L feed tank, a high pressure pump (provided up to 10 bar pressure), a pressure vessel to contain one flat sheet membrane featuring an active membrane surface area (A) of 55.4 cm^2 and an electrical control panel. The desired operating pressure was achieved by adjusting the valves located in the retentate and permeate streams, and by setting the digital pressure switch to the required pressure. A cross-flow RO system is shown in Figure 2.

The performance of EoL membranes was examined with respect to permeate flux and salt rejection using four different membrane sheets (EoL-M1, EoL-M2, EoL-M3, and EoL-M4). All tests were performed in the cross-flow RO system at 10 bar (Figure 2). All tested RO membranes were initially soaked in deionized water for 24 h prior to any further testing. For all experiments, the system was allowed to

stabilize for 1 h before recording any results. The permeate flux (J) was calculated using Equation 1 [20], by measuring the volume of water collected during 10 minutes interval Δt, where the active membrane surface area (A) was 55.4 cm^2.

$$J = \frac{Q}{\Delta t\, A} \quad (1)$$

Where J is the permeate flux ($L/m^2.s$), Q is the permeating volume (L), A is the membrane area (m^2) and Δt is the time interval (s).

Salt rejection is calculated using the following formula [3]:

$$R = 100\% \left(1 - \frac{C_p}{C_0}\right) \quad (2)$$

Where R is the salt rejection (%), C_p and C_0 are the salt concentrations (mg/L) in permeate and feed water streams, respectively. Salt concentration was measured using a conductivity meter. Permeate volume and TDS readings were recorded every 10 minutes for 90 minutes filtering time.

2.3.1 Membrane Performance Characterization using Deionized Water and Synthetic NaCl Solution

Permeate flux of the EoL membranes and commercial BW30 and NF90 membranes was first tested using deionized water. Secondly, permeate flux and salt rejections of these membranes were tested using 5,000 mg/L synthetic NaCl at the same operating pressure of 10 bar.

2.3.2 Removal of different Salts (NaCl, Na_2SO_4, $MgSO_4$ and $MgCl_2$) by EoL Seawater RO Membranes

The removal of (NaCl, Na_2SO_4, $MgSO_4$ and $MgCl_2$) salts was investigated using one flat sheet EoL seawater RO membrane (EoL-M1) following the procedure above to assess the ability of EoL membranes to remove the most common salts found in seawater and natural brackish water.

2.3.3 Removal of Humic Acid by EoL Seawater RO Membranes

The ability of EoL membranes to remove natural organic matter was assessed using 10 mg/L humic acid. After 1 h stabilization, a permeate sample was collected every 30 minutes up to 90 minutes. Permeate flux and HA concentration was obtained for each collected sample. Ultraviolet-visible (UV-Vis) spectrophotometer (Ocean Optic, USB4000) was used to determine HA absorbance of all samples at 200 nm to 800 nm wavelengths using 3.5 ml from each sample. Deionized water was used as a reference for all tested samples. Rejection of HA was calculated using Equation 2.

2.3.4 Evaluation of EoL Membranes Performance for Brackish Water Treatment

In this part, natural brackish water treatment was investigated by the direct reuse of the EoL SWRO membranes in the cross flow RO system. The used brackish water (5000 mg/L) was supplied from Al Khoudh area (Oman) ground water. Brackish water filtration was first performed directly without pretreatment in order to investigate the ability of EoL seawater RO membranes to deal with brackish water as a single treatment method. Then, brackish water was initially filtered by microfiltration (0.45 μm filter) as a pretreatment step before conducting RO filtration with old membranes.

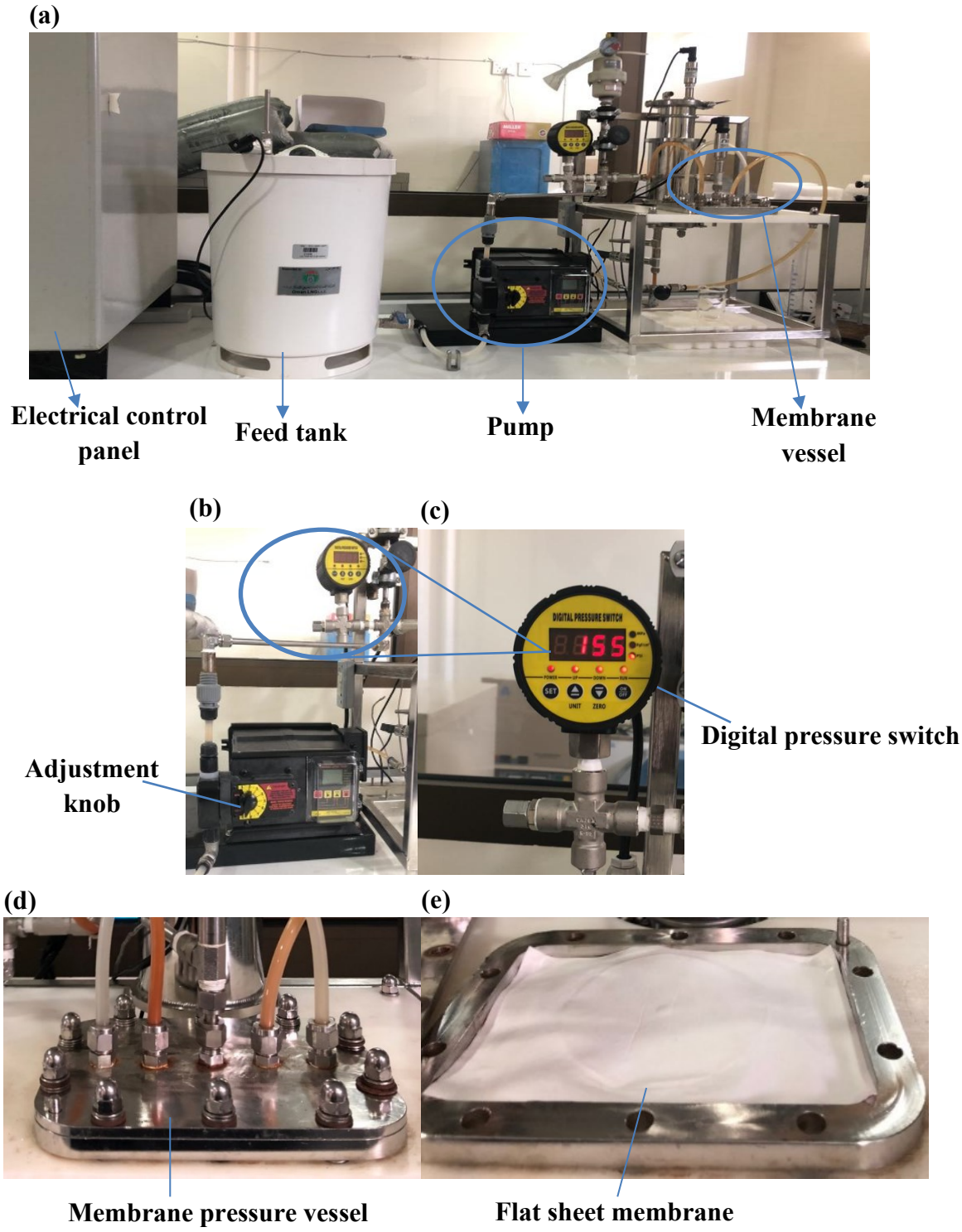

Figure 2 (a) Cross-flow filtration setup used for evaluation of EoL RO membranes performance, (b and c) Pump and digital pressure switch, (d and e) Membrane vessel and flat sheet membrane

3.0 RESULTS AND DISCUSSION

3.1 EoL Membranes Surface Characterization

EoL RO membrane samples were imaged using FE-SEM (Field Emission Scanning Electron Microscopy) to investigate the changes in membrane surface morphology after the end of their lifetime and also after the cleaning process. EoL membrane images, along with an image of virgin SW30HR membrane for comparison. Energy dispersive X-ray spectroscopy (EDS) was coupled with SEM analysis to examine the chemical content of the membranes surface. Results are shown in Figure 3.

Based on the SEM images and the EDS spectra of the aged membranes [Figure 3 (b, c, d and e)], various types of deposits, i.e., Na, Cl, Mg, Al and Si, are observed in the end-of-life membranes surface before cleaning which were due to RO desalination process. Moreover, sulphur observed in the EDS spectra for all the membranes is a characteristic of the polysulfone support layer [17]. SEM micrographs of the EoL membranes after cleaning [Figure 3 (f, g, h and i)] show less contaminants compared to the EoL membranes before cleaning and are approximately similar to that of a virgin SW30HR membrane (Figure 3a). The use of the combined chemical cleaning process was shown to be effective for removing these deposits from the surface of EoL-M1 and EoL-M4 membranes as shown by Energy-dispersive X-ray spectroscopy results. EDS of EoL-M1 and EoL-M4 are similar to the EDS observed for virgin SW30HR membrane (Figure 3a). EDS analysis of EoL-M2 and EoL-M3 membranes after cleaning [Figure 3 (g and h)] showed that membranes surface was much cleaner, however; fouling constituents were still detected from the surface of these membranes after the cleaning process. The main elemental composition of the membranes surfaces as detected in EDS spectrum 2 of both EoL-M2 and EoL-M3 were C, O, and S which were the most predominant elements and N, Si, Al, Mg and K that were only present in low concentrations, probably due to the incomplete removal of the fouling constituents during the cleaning process. Therefore, EDS analysis suggests that the fouling constituents remaining on the surface of EoL membranes after the cleaning processes included mixture of organic and inorganic materials.

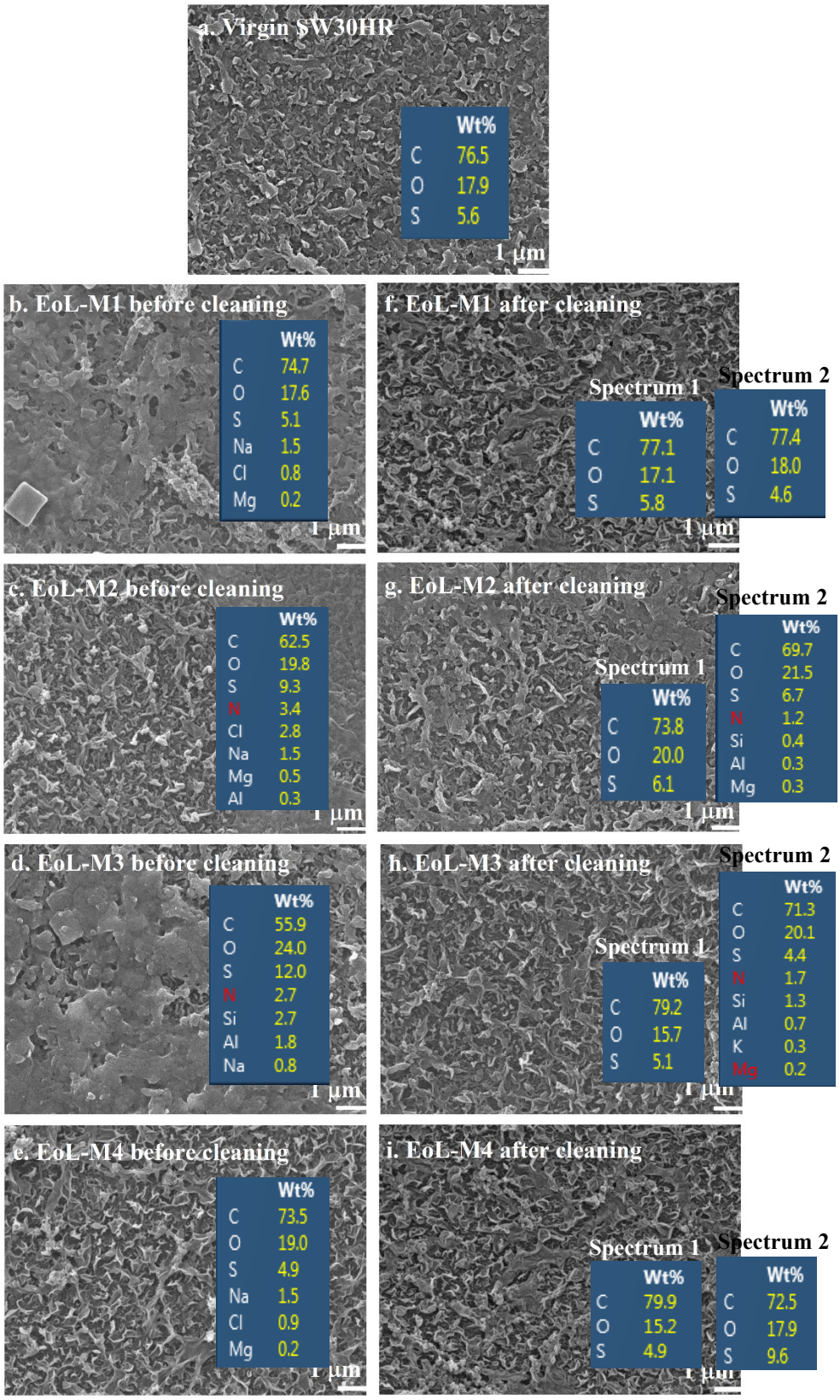

Figure 3 FE-SEM/EDS analysis of (a) virgin SW30HR RO membrane, and EoL seawater RO membranes (b, c, d and e) before and (f, g, h and i) after cleaning

The functional groups of the EoL membranes surface were identified by ATR-FTIR. Figure 4 a and b shows the FTIR spectra of the EoL membranes compared to a commercial SW30HR RO membrane. The spectra from the EoL membranes show a broad peak at 3310 cm^{-1} corresponding to free and hydrogen bonded N-H stretching [21]. The peaks at 2930-2970 cm^{-1} are assigned to aliphatic C-H bonds [22]. The peaks at 1665 cm^{-1} and 1543 cm^{-1} are representative of C=O and N-H stretching vibration of amide I and amide II from the thin polyamide layer. The peaks at 1609 cm^{-1}, 1488 cm^{-1} and 1448 cm^{-1} are related to C=C ring vibrations of polyamide [21]. The peaks at 1506 cm^{-1} and 1588 cm^{-1} were attributed to polysulfonyl group in the polysulfone porous supporting layer [23]. The prominent peak at 1242 cm^{-1} is assigned to C-O-C asymmetric stretching vibration in polysulfone [24]. No additional peak appeared and all spectra in aged membranes are consistent with the commercial SW30HR RO membrane which indicates that there are no changes in the chemical structure of the tested EoL RO membrane samples across the entire spectra. However, aged membranes spectra in wavenumber at 3310 cm^{-1} (Figure 4a) and wavenumber between 1400 to 1800 cm^{-1} (Figure 4b) represent small reduction in the intensity of N-H, C=C and C=O peaks compared to the spectrum of virgin SWRO membrane, this indicates that the top layer of aged membranes starts to degrade as a result of continuous filtration and cleaning process.

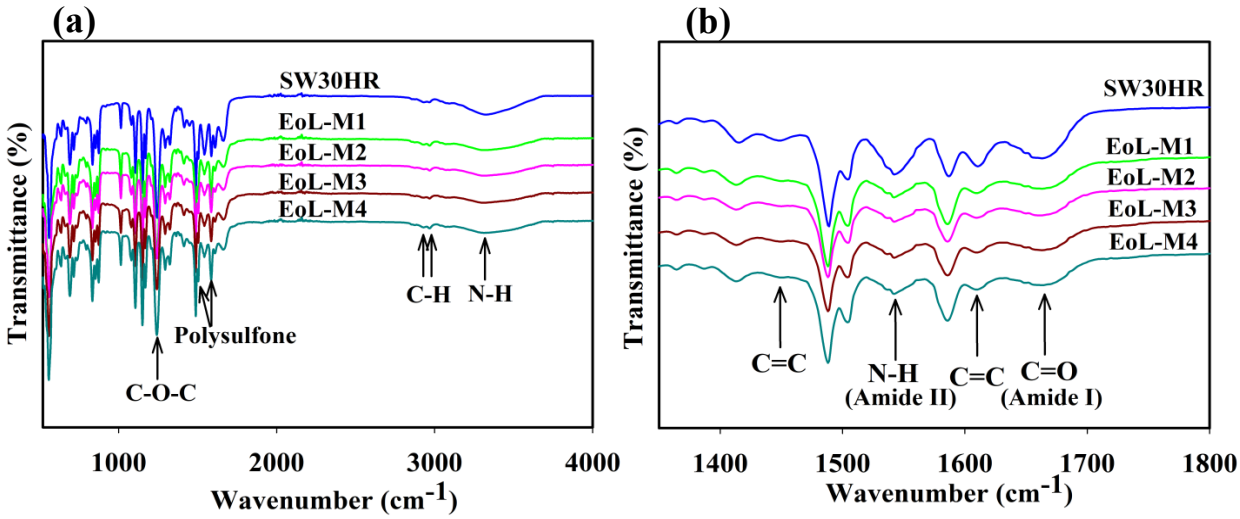

Figure 4 ATR-FTIR spectra of commercial SW30HR RO membrane and EoL SWRO membranes (a) wavenumber ranged between 520 and 4000 cm^{-1} and (b) wavenumber ranged between 1400 and 1800 cm^{-1}

Thermogravimetric analysis (TGA) results of the virgin and the EoL membranes are shown in Figure 5a. All TGA curves showed similar behavior in which two main weight loss regions were observed. The initial temperature of decomposition was detected between 370 and 440 °C and is attributed to the polymer degradation [25, 26]. The second stage of decomposition (from 470-550 °C) is due to backbone cleavage of the polymer [25]. A very small weight loss can be observed at 250 °C may be attributed to the removal of the remaining organic fouling contaminants on the membrane surface

after the cleaning process. However, a slightly more weight loss can be observed for EoL-M3 between 320-400 °C and for EoL-M1 and EoL-M4 (between 450-550 °C, inset in Figure 5a) which indicates that these membranes are less stable compared to the virgin SW30HR RO membrane because of the fouling.

Water contact angle (WCA) values observed for the end-of-life membranes are shown in Figure 5b. All end-of-life membranes showed contact angle values lower than 90°. WCA values of EoL-M1 (51° ± 5°), EoL-M2 (38° ± 4°) and EoL-M4 (50° ± 3°) are lower than the SW30HR (59° ± 3°) except EoL-M3 (85° ± 3°). The lower WCA values for EoL-M1, EoL-M2 and EoL-M4 probably due to the inorganic foulant or biofilm form at the membranes which cannot be completely removed, or a slight degradation of the membranes after the continuous filtration and cleaning process. Contradictory result of higher WCA value for EoL-M3 is obtained owing to the domination of organic foulant which may change the surface chemistry of EoL-M3. Although the WCA results for EoL-M1 and EoL-M4 are comparable, the lowest WCA value for EoL-M2 and the highest for EoL-M3 are probably due to the inefficient cleaning method that removed only part of the inorganic and carbon-based organic fouling constituents. The domination of carbon-based organic fouling constituents in EoL-M3 was confirmed by observing the increased carbon content (71.3 Wt %, Figure 3h) for EoL-M3 when compared to EoL-M2 (69.7 Wt %, Figure 3g) in EDS analysis. Typically, a droplet contact angle measurement of less than 90° will classify a membrane surface as hydrophilic. The lower the contact angle the greater the tendency for water to wet the surface and the higher the hydrophilic character and the permeate flux [27].

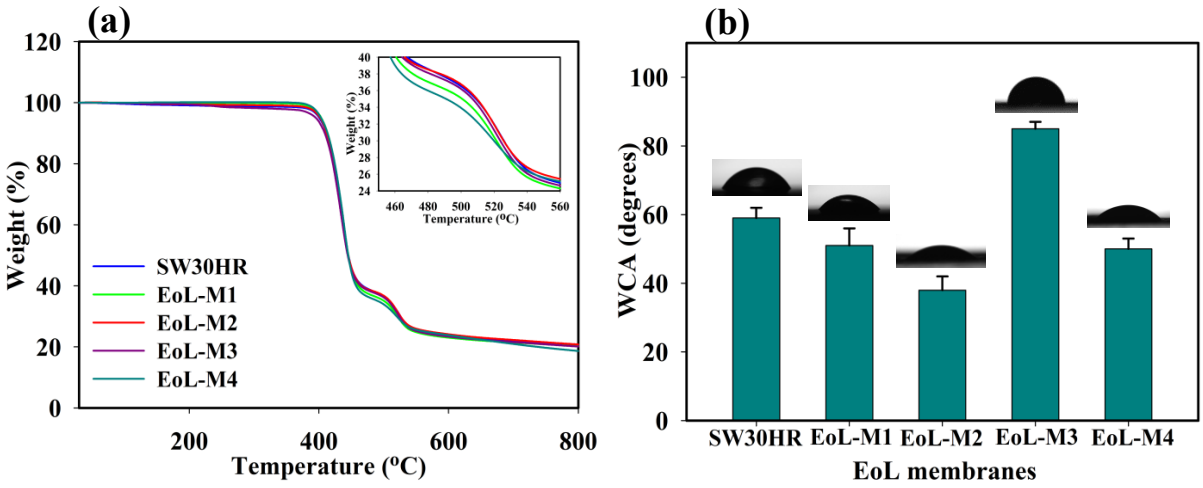

Figure 5 (a) TGA graph of commercial SW30HR RO membrane and EoL SWRO membranes, inset is temperature range between 450 and 550 °C and (b) WCA of commercial SW30HR RO membrane and EoL SWRO membranes

XPS measurement was conducted to verify the elemental composition and surface properties of the virgin (SW30HR) and the tested end-of-life membranes (EoL-M1 – EoL-M4). XPS is a unique surface-sensitive technique that detects electrons originated only from the top few nanometers (~10 nm).

Therefore, the elemental information of only the upper PA layer can be attained for all membranes. XPS survey spectra in Figure 6 show predominant peaks of C 1s at 284.6 eV, N 1s at 399.7 eV, O 1s at 532.2 eV acquire from the aromatic poly amide (PA) seawater RO membranes [28]. The additional Na 1s at 1072.6 eV is detected in the virgin sample due to the membrane's storage in a preservative agent like sodium meta-bisulfite before use in the RO desalination process. The combined chemical cleaning process can effectively remove the fouling constituents on the surface for all EoL membranes and no additional peaks are detected.

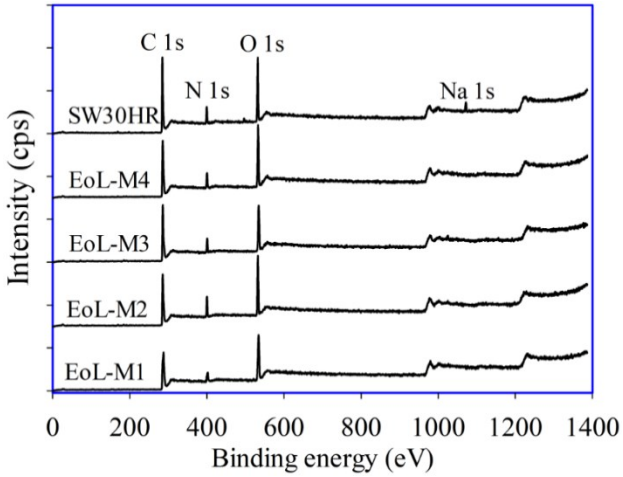

Figure 6 XPS survey spectra of membrane samples: EoL-M1, EoL-M2, EoL-M3, EoL-M4 and SW30HR

The chemical environment of C 1s element is further studied by deconvoluting of C 1s for virgin and EoL-M1 – EoL-M4 membranes. High resolution XPS spectra of core level C 1s peaks for the virgin and EoL-M4 are shown in Figure 7a and b and other C 1s deconvoluted membrane samples (EoL-M1, EoL-M2 and EoL-M3) were shown in Table S2 (supporting information). C 1s spectrum for the virgin membrane (Figure 7a) can be deconvoluted into three components at 284.6 eV, 286.1 eV and 287.8 which can be attributed to C-C/C-H from aliphatic and aromatic bonds, C-O/C-N from part of the amide bonds and C=O from carbonyl groups of carboxylic acid and amides, respectively. For EoL-M4 membrane (Figure 7b), the binding energies at 284.6 eV, 286.0 eV and 287.7 eV can be assigned to C-C/C-H, C-O/C-N and C=O bonds [29]. In EoL-M4 membrane, the amount of C−C/C-H was reduced substantially from 66.2% (the virgin) to 50.3% and an increase in C=O from 7.5 % (the virgin) to 20.4% were due to the formation of inorganic and organic foulant at membrane surface.

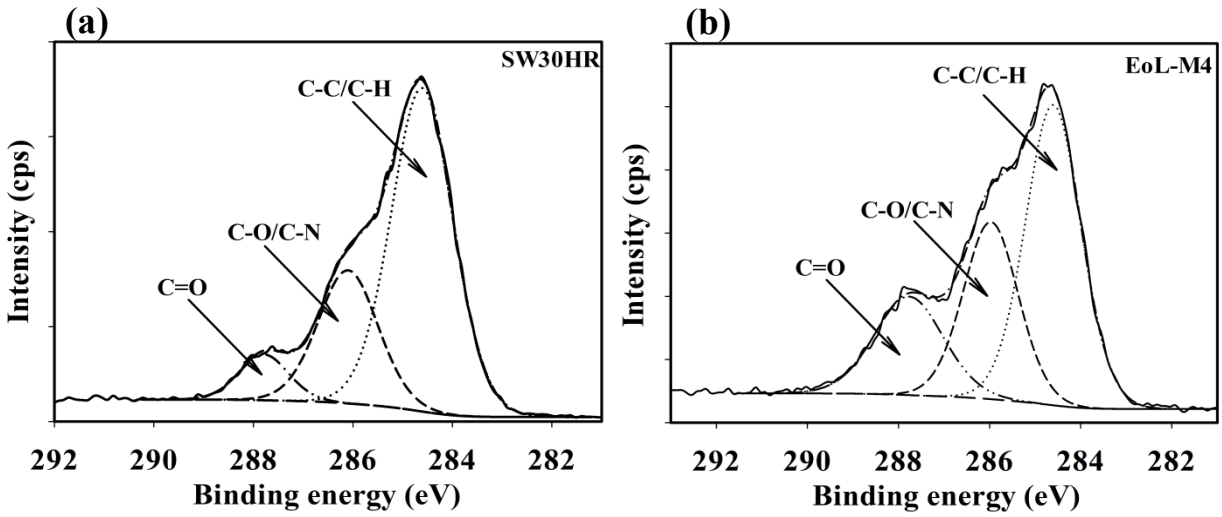

Figure 7 High-resolution XPS spectra of C1s for (a) SW30HR and (b) EOL-M4 membranes

3.2 EoL Membranes Performance Characterization: Deionized Water and synthetic NaCl Solution

The performance of EoL membranes and commercial BW30 & NF90 membranes were investigated in terms of water flux and salt rejection in a cross-flow RO system using deionized water and synthetic NaCl solution (5,000 mg/L). Figure 8 shows the resulting pure water flux (L/m^2.h) versus filtering time (minutes) for all tested membranes. The obtained flux was approximately constant with time for all membranes; this indicates that there was no leakage within the RO system. Among the old membranes, EoL-M1 shows the highest permeate flux (17.6 L/m^2.h) while EoL-M3 shows the lowest value (6.5 L/m^2.h). This result can be explained based on water contact angle measurements of EoL membranes as shown in Figure 5b. EoL-M3 presented lower hydrophilic character because its contact angle value was higher compared to EoL-M1, EoL-M2 and EoL-M4 membranes. Therefore, EoL-M3 has the lowest permeate flux compared to the other two membranes. On the other hand, in spite of the highest hydrophilicity of the EoL-M2 membrane (lower contact angle), EoL-M1 was found to have the highest permeate flux of 17.6 (L/m^2.h). This is probably due to the membrane fouling that can decrease the contact angle when crystalline structures or biofilms form, leading to a decline in permeate flux [30].

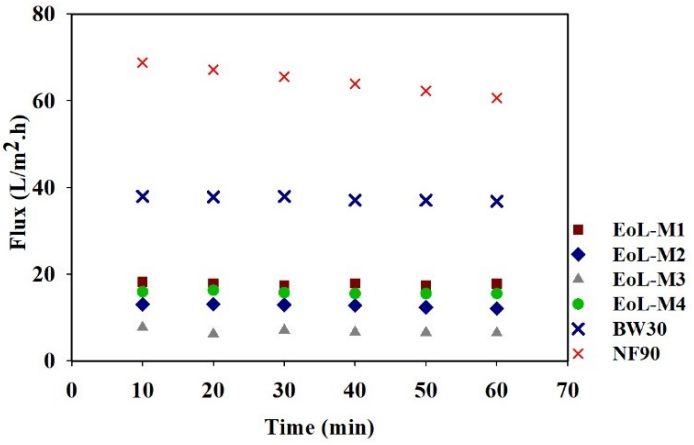

Figure 8 Deionized water flux of EoL membranes & commercial BW30 and NF90 membranes at 10 bar

Figure 9 shows permeate flux values obtained with time for all tested membranes using 5,000 mg/L NaCl feed solution. When comparing the permeate flux of EoL membranes with BW30 and NF90 membranes; results show that permeate flux of old membranes is around 60% and 65% lower than BW30 and NF90 membranes (Figure 9), respectively. This indicates that EoL membranes could be utilized for lower scale applications like small-scale RO systems. Another suggestion is to use these membranes at a relatively higher operating pressure, to increase the rate of water production, in lower grade applications like selective demineralization of brackish water and wastewater treatment. This is especially interesting for those processes which require low-cost membranes due to a high membrane replacement rate [31]. Overall, it is evident that all reused RO membranes will feature varying hydraulic performances, which will need to be considered when identifying reuse applications.

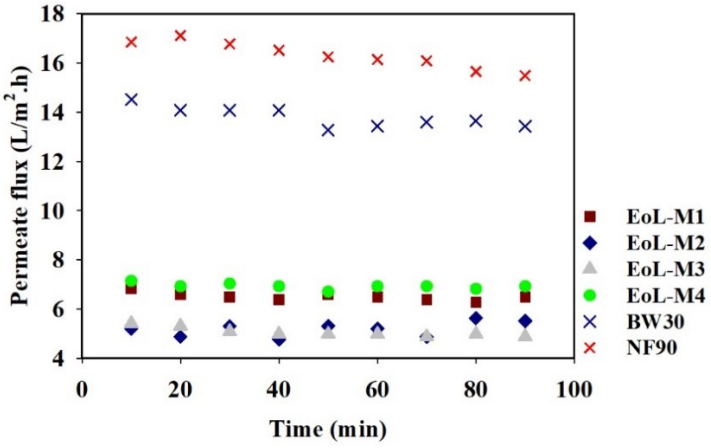

Figure 9 Flux of EoL RO membranes compared to commercial BW30 and NF90 membranes using 5,000 mg/L NaCl feed solution

Figure 10 shows rejection performance of the same membrane samples with time. NaCl rejection obtained using EoL-M1, EoL-M2, EoL-M3, and EoL-M4 membranes were in the range of 84-92%. EoL membranes presented higher salt rejection than commercial BW30 and NF90 membranes (salt rejection was around 80% in case of commercial BW30 membrane and around 65% in case of NF90 membrane). These results showed a great promise of the direct reuse of the EoL SWRO membranes for lower specification applications. Compared to commercial NF membranes, end-of-life RO membranes are less-expensive alternative for water purification. The application of EoL membranes for brackish water desalination was tested during the experimental work and results will be discussed in section 3.5.

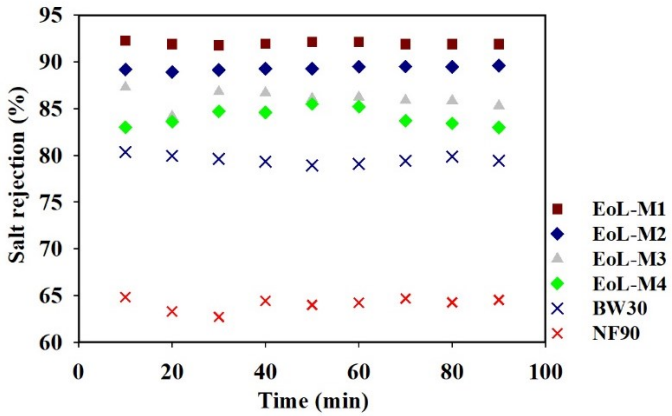

Figure 10 Rejection of EoL RO membranes compared to commercial BW30 and NF90 membranes using 5,000 mg/L NaCl feed solution

3.3 Removal of Common Salts (NaCl, Na_2SO_4, $MgSO_4$ and $MgCl_2$) by EoL Seawater RO Membranes

The removal of single salts of NaCl, Na_2SO_4, $MgSO_4$ and $MgCl_2$ from their aqueous solutions was investigated using EoL-M1 membrane. EoL-M1 was investigated because it showed the highest NaCl rejection as shown in the previous section. As shown in Figure 11, the highest rejection was achieved for Na_2SO_4 (85.8%) and NaCl (84.1%) while rejection of $MgCl_2$ was the lowest (50%) and rejection of $MgSO_4$ was moderate (70%). This sequence can be explained based on solute transport mechanisms including; charge effects (Donnan exclusion mechanism, which is often used to explain the influence of membrane charge on the retention of ions) and/or diffusion and molecular size exclusion of the salts. These results are in accordance with the Donnan theory (for negatively charged membranes) except for sodium chloride that was expected to have lower rejection than $MgSO_4$. The unexpected high rejection of NaCl can be explained by the contribution of diffusion on the transport of solutes through the membrane. On the basis of diffusivity; Gallab *et al*. [32] found that at high feed concentrations ($\geq$ 5,000 mg/L), the mass transfer coefficient (k, (m/s)) for magnesium salts was higher than that of sodium salts (Table 1), subsequently lower rejection was obtained for magnesium salts as a result of the higher diffusivity of magnesium, despite of its larger hydrated ionic radius (Table 2).

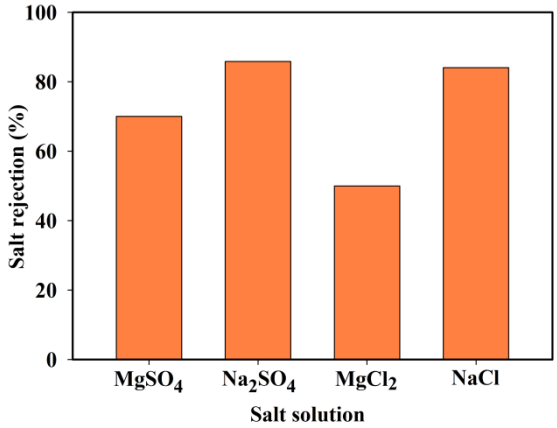

Figure 11 Salt rejection of each salt solution of 5,000 mg/L by EoL-M1 membrane at 10 bar

A little increase in the retention of Na_2SO_4 than NaCl is caused by size effects of the sulphate and chloride anions, where SO_4^{2-} has a larger hydrated radius compared to Cl^- as shown in Table 2. Moreover, Labbez *et al*. [33] showed that rejection of ions by PA membranes is often controlled by the affinity of the membrane material for charged ions which determined its fixed charged and thus its ability for ionic retention. In other words, each ion could have its individual contribution to the surface charge of the membrane by the means of adsorption. For example, he showed in the same study that a membrane gains a positive charge in presence of $MgSO_4$ and $MgCl_2$ and a negative charge in presence of KCl and K_2SO_4. However, because of the stronger adsorption of membrane for chloride ions compered to sulphate ions, the effective membrane volume charge is much stronger for KCl solution than for K_2SO_4 solution [33]. This result explains the reduced rejection percent of NaCl compared to Na_2SO_4 and equivalent to the case of $MgCl_2$ and $MgSO_4$. Therefore, it is clear that prediction of salts rejection by organic membranes becomes very specific and complicated.

Table 1 Mass transfer coefficient for different salts at 5,000 mg/L [32]

Salt (5,000 mg/l)	K (m/s) × 10^{-2}
NaCl	1.23
Na_2SO_4	1.28
$MgSO_4$	1.43

Table 2 Ionic and hydrated ionic radii of the studied ions [32]

Ion	Ionic radius (nm)	Hydrated ionic radius (nm)	Hydration energy (kJ mol^{-1})
Na^+	0.095	0.365	407
Mg^{2+}	0.074	0.429	1921
Cl^-	0.181	0.347	376
SO_4^{2-}	0.23	0.38	1138

The permeate flux obtained each 10 minutes during 90 minutes filtration of four salt solutions is illustrated in Figure 12. The permeate flux obtained for Na_2SO_4, NaCl, and $MgSO_4$ was approx. 7.8-8.6 L/m^{2}h, while the flux of $MgCl_2$ was approx. 11 L/m^{2}h. Usually, high salt rejection is achieved at the expense of low flux and vice versa [1]. Overall, EoL-M1 exhibited excellent rejection of different salts with reasonable flux which gives a good indication of the capability of EoL membranes to reject the major of common salts in seawater and brackish water. Hence, EoL RO membranes can be directly used in different applications including seawater pretreatment and water purification.

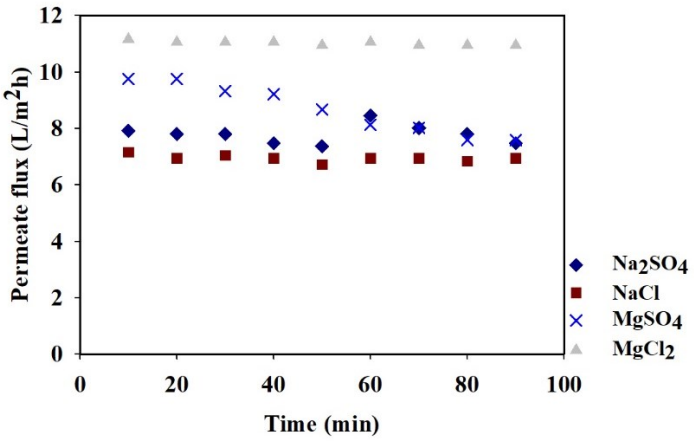

Figure 12 Permeate flux of 5,000 mg/L salts observed using EoL-M1 membrane at 10 bar

3.4 Humic Acid Removal

The performance of the directly used EoL membranes (EoL-M1, EoL-M2, EoL-M3 and EoL-M4) was also studied using 10 mg/L humic acid solution at 10 bar. Feed and permeate solutions were analyzed by UV-Vis spectroscopy in the wavelength range of 200 to 800 nm. Predicted absorbance values were converted to concentrations where HA rejection was obtained using (C_p/C_o) ratio. Figure 13 shows the calculated HA rejection and filtrate flux of samples collected during 30 minutes after two hours of continued filtration. Results indicate that all of the reused membranes showed excellent HA rejection reaching 99.6% for some filtrate samples. Therefore, EoL seawater RO membranes can be utilized in pretreatment section of water treatment plants to overcome fouling problems by removing a high fraction of natural organic matter (NOM) and other contaminants from feed water. Moreover, the difference in permeate flux obtained using different EoL membranes was discussed in section 3.2. In addition, it was found that the flux of humic acid (23 L/m^{2}h) is higher than the flux values obtained for different salt solutions (6-11 L/m^{2}h) using EoL-M1 as shown in previous section. This is due to the higher concentration of feed in case of synthetic salts filtration (5,000 mg/L) which results in higher osmotic pressure and this leads to higher flux resistance. Thus, permeation flux decreases with increasing of salts or organics concentration contained in feed water.

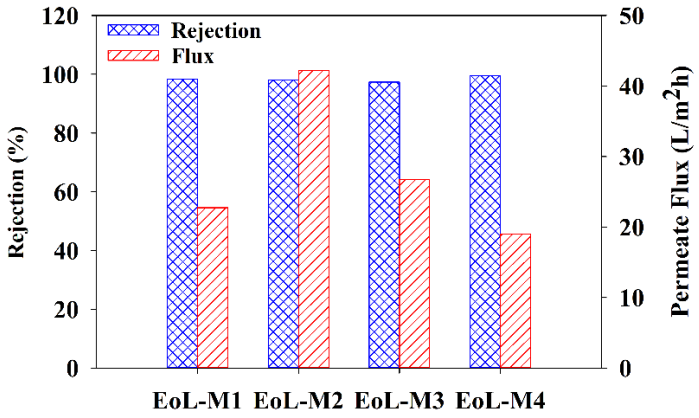

Figure 13 Rejection and permeate flux of HA obtained by filtration of 10 mg/L HA feed using four EoL membranes

3.5 Direct Reuse of EoL Membranes for Brackish Water Treatment

EoL seawater RO membranes were used for natural brackish water treatment in order to validate the ability of directly reused EoL membranes for brackish water treatment. Brackish water filtration was first assessed without any pretreatment, and then pretreatment of brackish water was performed using vacuum filtration (0.45 μm membranes). A detailed analysis of the brackish water sample (groundwater) collected from Al Khoudh area in Oman can be found in Table S3 in the supporting information.

3.5.1 Without Pre-treatment

Figure 14 shows that permeate flux observed for 5,000 mg/L brackish water filtration by EoL membranes have lower values compared to commercial BW30 and NF90 membranes. The permeate flux of EoL-M1 and EoL-M4 was 20 and 50% lower than the flux values obtained for BW30 and NF90 membranes, respectively. While the flux of EoL-M2 and EoL-M3 membranes was around 50 and 64% lower than the flux obtained for the commercial BW30 and NF90 membranes at the same operating conditions, respectively. Seawater RO membranes have lower flux compared to brackish water RO membranes because the surface of SWRO membranes contains more hydrophilic groups (-COOH) and presents lower roughness than BWRO membranes [34].

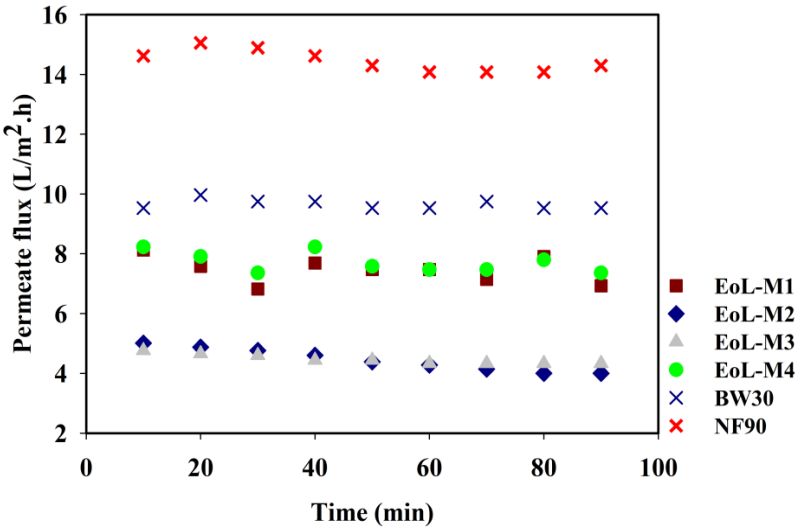

Figure 14 Flux of old RO membranes compared to commercial BW30 and NF90 membranes using 5,000 mg/L BW feed

Salt rejection of all membranes was tested using 5000 mg/L brackish water, results are illustrated in terms of salt rejection and total dissolved solids (TDS) in Figures 15 a and b, respectively. Rejection of EoL membranes (75-77%) was within the commercial NF90 membrane rejection performance (which showed a rejection of 77%) except for EoL-M2. Salt rejection values obtained for EoL-M2 were intermediate between the commercial BW30 and NF90 membranes. Product water by old membranes presents TDS values between 800-1300 mg/L, which are within the permissible limit of irrigation water (500-2000 mg/L [35]). Therefore, the product water of BW filtration by EoL SWRO membranes can be used for irrigation purposes to cover the agricultural water demand. This practice will reduce the overall cost of irrigation by producing water suitable for crop irrigation with lower cost of filtering elements (compared to the higher cost of commercial BWRO and NF90 membranes). Moreover, in some cases, desalinated water has to be adapted to the crop and soil requirements by blending with raw water stream.

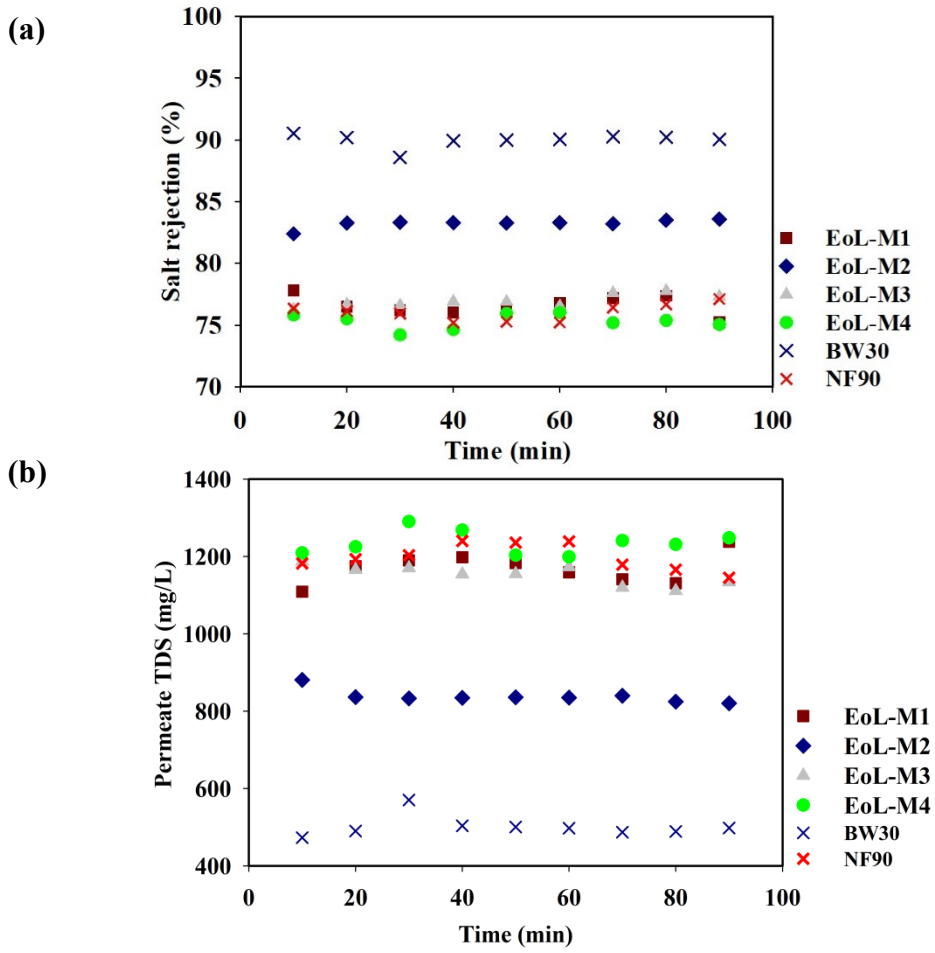

Figure 15 (a) Salt rejection and (b) TDS values obtained for EoL membranes and the commercial BW30 and NF90 membranes using (5,000 mg/L) brackish water at 10 bar

3.5.2 After Pretreatment

Figures 16 a and b show water flux and salt rejection obtained using EoL-M2 before and after brackish water pretreatment. As it can be observed from these figures, following the pretreatment step, permeate flux and salt rejection have slightly increased. This increment occurred as a result of removing part of the insoluble and suspended impurities from the raw water stream that causes membrane fouling. However, permeate flux and salt rejection have only increased by 5-15%. This result suggests that the EoL RO membranes could potentially be used for lower specification applications with little or no treatment depending on the raw water characteristics and the required product quality. Moreover, the difference in the hydraulic performance of old membranes due to the pretreatment step might be significant in long term processes.

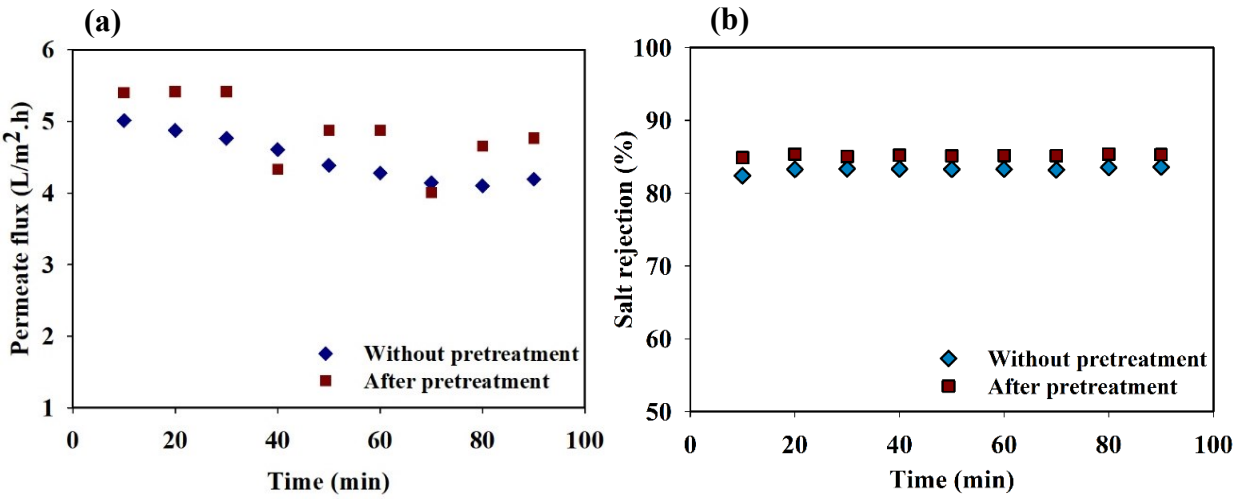

Figure 16 (a) Permeate flux and (b) Salt rejection of EoL-M2 membrane using 5,000 mg/L brackish water feed before and after pretreatment

4.0 CONCLUSIONS

Large stocks of EoL RO membranes have been accumulated over the years and their management should be considered as an important action for the sustainability of RO technology/industry. The main objective of this study was to validate the possibility of direct reuse of the EoL SWRO membranes for water treatment without any membrane treatment or modification that would add to the operational costs (OPEX). Permeate flux and salt rejection of four different EoL membranes (EoL-M1, EoL-M2 EoL-M3 and EoL-M4) were tested using different feeds (Deionized water, NaCl solution (5,000 mg/L) and natural brackish water (5,000 mg/L)) at 10 bar, results of these membranes were compared with the performance of two commercial membranes (BW30 and NF90). Moreover, removal of common salts found in natural water sources (Na_2SO_4, Mg_2SO_4 and $MgCl_2$) and humic substances (HS) was also investigated. Moreover, EoL membranes were characterized by TGA, FTIR, SEM, WCA and XPS techniques. It was shown that 84-92% NaCl rejection was achieved by end-of-life SWRO membranes. Excellent rejection of different salts [Na_2SO_4 (85.8%), NaCl (84.1%), $MgSO_4$ (70.0%) and $MgCl_2$ (50.0%)] was exhibited by EoL-M1, while approximately complete rejection was achieved for humic acid. The permeate water quality observed by using EoL membranes for brackish water filtration showed salt concentrations in the range of 800-1300 mg/L, which was within the permissible limit of agriculture water. These results are encouraging, in particular for Oman where the farmers are facing the challenging salinization of their groundwater, and therefore there is an increasing demand for brackish water desalination. Hence, the potential reuse of EoL RO membranes will contribute to meeting the demands of these farmers.

ACKNOWLEDGEMENT

The authors express gratitude to the Nanotechnology Research Center, Sultan Qaboos University, Oman for their support to accomplish the research work that led to the success of this

project. The authors would like to acknowledge the Central Analytical and Applied Research Unit (CAARU) at the College of Science for their help. We also wish to thank the Department of Physics, College of Science for FESEM/EDS and XPS measurement and the Department of Mechanical, College of Engineering for their help in RO modules dismantling. The authors also would like to thank financial support from His Majesty Trust Fund (HMTF) under grant numbers SR/ENG/PCED/17/01.

CONFLICTS OF INTEREST

The authors declare that there is no conflict of interest regarding the publication of this paper.

REFERENCES

[1] M. M. Schenkeveld, R. Morris, B. Budding, J. Helmer, S. Innanen. (2004). Seawater and Brackish water desalination in the Middle East, North Africa and Central Asia: A review of key issues and experiences in six countries, *Relatório técnico, Banco Mundial, Nimes, França.*

[2] R. García-Pacheco, J. Landaburu-Aguirre, P. Terrero-Rodríguez, E. Campos, F. Molina-Serrano, J. Rabadán, D. Zarzo, E. García-Calvo. (2018). Validation of recycled membranes for treating brackish water at pilot scale. *Desalination*, *433*, 199–208.

[3] H. Dach. (2008). Comparison of nanofiltration and reverse osmosis processes for a selective desalination of brackish water feeds.

[4] G.-d. Kang, Y.-m. Cao. (2012). Development of antifouling reverse osmosis membranes for water treatment: A review. Water research, *46,* 584–600.

[5] S. S. Shenvi, A. M. Isloor, A. Ismail. (2015). A review on RO membrane technology: developments and challenges. *Desalination*, *368*, 10–26.

[6] S. F. Anis, R. Hashaikeh, N. Hilal. (2019). Reverse osmosis pretreatment technologies and future trends: A comprehensive review. *Desalination, 452*, 159–195.

[7] A. E. Anqi, N. Alkhamis, A. Oztekin. (2015). Numerical simulation of brackish water desalination by a reverse osmosis membrane. *Desalination, 369,* 156–164.

[8] W. Lawler, Z. Bradford-Hartke, M. J. Cran, M. Duke, G. Leslie, B. P. Ladewig, P. Le-Clech. (2012). Towards new opportunities for reuse, recycling and disposal of used reverse osmosis membranes. *Desalination*, *299*, 103–112.

[9] S. Molina, J. Landaburu-Aguirre, L. Rodríguez-Sáez, R. García-Pacheco, G. José, E. García-Calvo. (2018). Effect of sodium hypochlorite exposure on polysulfone recycled UF membranes and their surface characterization. *Polymer Degradation and Stability*, *150,* 46–56.

[10] W. Lawler, A. Antony, M. Cran, M. Duke, G. Leslie, P. Le-Clech. (2013). Production and characterisation of UF membranes by chemical conversion of used RO membranes. *Journal of Membrane Science*, *447*, 203–211.

[11] W. Lawler. (2015). Assessment of end-of-life opportunities for reverse osmosis membranes. School of Chemical Engineering and Faculty of Engineering.

[12] J. M. Veza, J. J. Rodriguez-Gonzalez. (2003). Second use for old reverse osmosis membranes: wastewater treatment. *Desalination, 157*, 65–72.

[13] J. J. Rodriguez, V. Jiménez, O. Trujillo, J. Veza. (2002). Reuse of reverse osmosis membranes in advanced wastewater treatment. *Desalination, 150*, 219–225.

[14] W. Lawler, J. Alvarez-Gaitan, G. Leslie, P. Le-Clech. (2015). Comparative life cycle assessment of end-of-life options for reverse osmosis membranes, *Desalination*, *357*, 45–54.

[15] F. Mohammadi, M. Sahraei-Ardakani, Y. M. Al-Abdullah, G. T. Heydt. (2019). Coordinated scheduling of power generation and water desalination units. *IEEE Transactions on Power Systems.*

[16] T. D. Oyoh. (2017). Desalination in water treatment and sustainability.

[17] E. O. Mohamedou, D. P. Suarez, F. Vince, P. Jaouen, M. Pontie. (2010). New lives for old reverse osmosis (RO) membranes. *Desalination*, *253*, 62–70.

[18] C. Prince, M. Cran, P. Le-Clech, K. Uwe-Hoehn, M. Duke. (2011). Reuse and recycling of used desalination membranes. *Proceedings of Oz Water'11,* Adelaide.

[19] E. Coutinho de Paula, M. C. S. Amaral. (2017). Extending the life-cycle of reverse osmosis membranes: A review. *Waste Management & Research, 35*, 456–470.

[20] A. Abuhabib, M. Ghasemi, A. W. Mohammad, R. A. Rahman, A. El-Shafie. (2013). Desalination of brackish water using nanofiltration: performance comparison of different membranes. *Arabian Journal for Science and Engineering, 38*, 2929–2939.

[21] N. Melián-Martel, J. J. Sadhwani, S. Malamis, M. Ochsenkühn-Petropoulou. (2012). Structural and chemical characterization of long-term reverse osmosis membrane fouling in a full scale desalination plant. *Desalination, 305*, 44–53.

[22] W. Lee, C. H. Ahn, S. Hong, S. Kim, S. Lee, Y. Baek, J. Yoon. (2010). Evaluation of surface properties of reverse osmosis membranes on the initial biofouling stages under no filtration condition, *J. Membr. Sci., 351*, 112–122.

[23] C. J. Gabelich, K. P. Ishida, F. W. Gerringer, R. Evangelista, M. Kalyan, I. H. M. Suffet. (2006). Control of residual aluminum from conventional treatment to improve reverse osmosis performance. *Desalination, 190,* 147–160.

[24] K. Singh, S. Devi, H. C. Bajaj, P. Ingole, J. Choudhari, H. Bhrambhatt. (2014). Optical resolution of racemic mixtures of amino acids through nanofiltration membrane process. *Sep. Sci. Technol., 49*, 2630–2641.

[25] A. U. H. Khan, Z. Khan, I. H. Aljundi. (2017). Improved hydrophilicity and anti-fouling properties of polyamide TFN membrane comprising carbide derived carbon. *Desalination, 420*, 125–135.

[26] S. Javed, I. H. Aljundi, M. Khaled. (2017). High fouling-resistance of polyamide desalination-membrane modified with PEI/PAH polyelectrolyte multilayers. *Journal of Environmental Chemical Engineering*, 54594–4604.

[27] M. Liu, D. Wu, S. Yu, C. Gao. (2009). Influence of the polyacyl

chloride structure on the reverse osmosis performance, surface properties and chlorine stability of the thin-film composite polyamide membranes. *Journal of Membrane Science*, *326,* 205–214.

[28] A. Zirehpour, A. Rahimpour, A. Arabi Shamsabadi, M. Sharifian Gh, M. Soroush. (2017). Mitigation of thin-film composite membrane biofouling via immobilizing nano-sized biocidal reservoirs in the membrane active layer. *Environmental Science & Technology, 51*, 5511–5522.

[29] C. Wang, Z. Li, J. Chen, Y. Zhong, L. Ren, Y. Pu, Z. Dong, H. Wu. (2018). Influence of blending zwitterionic functionalized titanium nanotubes on flux and anti-fouling performance of polyamide nanofiltration membranes. *Journal of Materials Science, 53*, 10499–10512.

[30] E. Thomas, D. Muirhead. (2009). Impact of wastewater fouling on contact angle. *Biofouling, 25*, 445–454.

[31] R. García-Pacheco, W. Lawler, J. Landaburu, E. García-Calvo, P. Le-Clech. (2017). End-of-life membranes: Challenges and opportunities.

[32] G. Aas, A. Mea, S. Ha, A.-M. Msa. (2017). Effect of different salts on mass transfer coefficient and inorganic fouling of TFC Membranes.

[33] C. Labbez, P. Fievet, A. Szymczyk, A. Vidonne, A. Foissy, J. Pagetti. (2003). Retention of mineral salts by a polyamide nanofiltration membrane. *Separation and Purification Technology, 30*, 47–55.

[34] Y. Zhou, C. Gao. (2010). Comparison between BWRO membrane and SWRO membrane. *CIESC Journal*, *10*, 2590–2595.

[35] G. Fipps. (2003). Irrigation water quality standards and salinity management strategies. Texas FARMER Collection.

Table S1 Specifications of the commercial SW30HR, BW30 and NF90 membranes as provided by manufacturer (Dow filmtec membranes)

Membrane	**DOW BW30 RO Membrane**	**DOW NF90 Nanofiltration Membrane**	**DOW SW30HR RO Membrane**
Type	Standard	Low energy, low pressure	High rejection
Permeability ((L · h^{-1} · m^{-2}))/bar	44/18	78-102/9	29-40/55
pH range	2-11	2-11	2-11
Rejection	99.5% BW	99.0% $MgSO_4$ rejection	99.6%
Pore size/ MWCO	~100 Da	~200-400 Da	~100 Da
Polymer	Polyamide-TFC	Polyamide-TFC	Polyamide-TFC

Table S2 Quantitative analysis of individual carbon components on membrane sample surface using high resolution C 1s spectra

Sample	**% Concentration**		
	C-C/C-H	**C-O**	**C=O**
SW30HR	66.2	26.4	7.4
EoL-M1	34.6	45.3	20.1
EoL-M2	44.9	28.6	26.5
EoL-M3	52.4	22.8	24.8
EoL-M4	50.3	29.3	20.4

Brackish Water Sample (Groundwater) Characterizations

The brackish water sample (groundwater) collected from Al Khoudh area in Oman was analysed using a conductivity meter (Myron L Company Ultrameter II), a pH meter (a Mettler Toledo–Seven Compact pH/Ion Meter), alkalinity was determined using volumetric titration with 0.02 N sulphuric acid (H_2SO_4), total hardness of brackish water was determined using complexometric titration method with EDTA (total Hardness is defined as the sum of calcium and magnesium concentrations, expressed in mg/L), brackish water anions were determined using Metrohm Professional Compact Ion Chromatography system with Metrohm 858 Professional Sample Processor. A detailed analysis of the brackish water sample is shown below.

Table S3 Water quality parameters of the brackish water collected from Al Khoudh area in Oman

Parameter	Quantity
pH	8.04
Electrical Conductivity – uScm-1 (micro Siemens per centimeter)	9500
Color (Hazen Units)	< 5
Turbidity (NTU)	0.51
Total Dissolved Solids - mg/L	5035
Total Alkalinity – mg /L as CaCO3	230
Bicarbonate Alkalinity mg /L as CaCO3	230
Carbonate Alkalinity	0
Hydroxide Alkalinity	0
Total Hardness mg /L as CaCO3	1350
Calcium Hardness mg /L as CaCO3	116
Cations - mg/L	
Sodium	1728
Potassium	54
Calcium	46.3
Magnesium	259.1
Anions - mg/L	
Fluoride	0.46
Chloride	3090.3
Nitrite	Not detected
Bromide	16.8
Nitrate	48.7
Phosphate	Not detected
Sulphate	497.3